Phase Behavior of Monoglycerol Fatty Acid Esters in Nonpolar Oils: Reverse Rodlike Micelles at Elevated Temperatures

Lok Kumar Shrestha,[†] Takaaki Sato,[‡] Durga P. Acharya,[†] Tetsuro Iwanaga,[§] Kenji Aramaki,*[,†] and Hironobu Kunieda[†]

Graduate School of Environment and Information Sciences, Yokohama National University, Tokiwadai 79-7, Hodogaya-ku, Yokohama 240-8501, Japan, Division of Physics and Applied Physics, Faculty of Science and Engineering, Waseda University, Okubo 3−4−1, Shinjuku-ku, Tokyo 169-8555, Japan, and Interface Solution Division, Taiyo Kagaku Co. Ltd., Takara machi 1-3, Yokkaichi, Mie 510-0844, Japan

Received: January 27, 2006; In Final Form: May 1, 2006

We have studied nonaqueous phase behavior and self-assemblies of monoglycerol fatty acid esters having different alkyl chain lengths in different nonpolar oils, namely, liquid paraffin (LP 70), squalane, and squalene. At lower temperatures, oil and solid surfactants do not mix at all compositions of mixing. Upon an increase in the temperature of the surfactant system, the solid melts to give isotropic single or two-liquid phases, depending on the nature of the oil and the surfactant. All monolaurin/oil systems form an isotropic single-phase liquid, but with a decreasing alkyl chain length of surfactant, they become less lipophilic and immiscible in oils. As a result, a two-phase domain is observed in the oil rich region of all monocaprylin/oil systems over a wide range of concentrations. Judging from the phase diagrams, the surfactants are the least miscible with squalane, and the order of miscibility tendency is squalene > LP 70 > squalane. With a further increase of temperature, the solubility of the surfactant in the oil increases, and the two-liquid phase transforms to an isotropic single phase. This phase transformation corresponds to the reverse of the cloud-point phenomenon observed in aqueous nonionic surfactant systems. Small-angle X-ray scattering (SAXS) measurements show the presence of reversed rodlike micelles in the isotropic single phase, and the length of the aggregates decreases with increasing temperature and increasing alkyl chain length of the surfactant. These results indicate a rod−sphere transformation with increasing lipophilicity of the surfactant and confirms the validity of Ninham's penetration model in the reversed system. An addition of a small amount of water dramatically enhances the elongation of the reverse micelles. Increasing the surfactant concentration or changing the oil from squalene to LP 70 also increases the length of the rodlike aggregates.

1. Introduction

Surfactants form a variety of self-organized structures, such as micelles, vesicles, and many liquid crystals in water or oil or in both.[1] These self-organized structures influence the functions of surfactants to stabilize foams, emulsions, and solid suspensions. Conventional poly(oxyethylene) alkyl ethers or alkanoic-acid esters are most popular nonionic surfactants and are widely used in industrial, cosmetic, and household products. These surfactants form various self-organized structures in water, and their phase behavior has extensively been studied.[2−8] These self-organized structures are highly influenced by alkyl chain length, poly(oxyethylene) chain length, and temperature. However, since the poly(oxyethylene) hydrophilic moiety is soluble in many organic solvents, the surfactants have a tendency to dissolve monomerically in nonaqueous solvents, and hence it is practically difficult to form a variety of self-organized structures in the absence of water.[2] For these reasons the conventional surfactants are not efficiently used in the systems containing a large amount of oil because of high CMC or no CMC. On the other hand, most of the ionic surfactants are insoluble in many organic solvents, and they tend to be precipitated as a solid. Different from the conventional poly(oxyethylene) chains, other hydrophilic moieties such as sucrose, polyglycerol, and so on are more lyophobic,[9,10] that is, not soluble in many organic solvents. Hence, these hydrophilic, nonionic groups tend to aggregate even in nonpolar media, and it is possible to form different self-organized structures. Besides, the phase behavior in polyglycerol type nonionic surfactant systems is not largely influenced by temperature.[11−15] Polyglycerol fatty acid esters are the edible surfactants and mostly used in food, pharmacy, and cosmetics. Therefore an understanding of phase behavior study is of technological importance.

Recently we have studied the binary phase behavior of a homologous series of diglycerol fatty acid ester surfactants in different organic solvents.[16] These surfactants interestingly formed lamellar liquid crystal (L_α) after the melting of the solid (L_β) phase over a wide range of compositions. After melting of the L_α phase, isotropic reverse micellar solutions were reached depending on the nature of surfactant and oils. Compared to the diglycerol fatty acid esters, hydrophilic moiety of the monoglycerol fatty acid esters is almost half, such that the lipophilic character of the surfactant increases, and it may or may not form self-organized structures in the organic solvents. To our knowledge, there have been little studies on the phase behavior of these surfactants in organic solvents.

* To whom correspondence should be addressed. E-mail: aramakik@ynu.ac.jp. Phone and fax: +81-45-339-4300.
[†] Yokohama National University.
[‡] Waseda University.
[§] Taiyo Kagaku Co. Ltd.

10.1021/jp060587p CCC: $33.50
Published on Web 06/06/2006

SCHEME 1: Schematic Molecular Structure of Glycerol α-Monolaurate (Monolaurin), Squalane, and Squalene

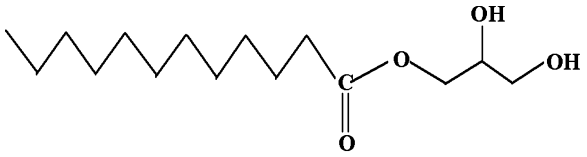

Glycerol α-monolaurate (Monolaurin)

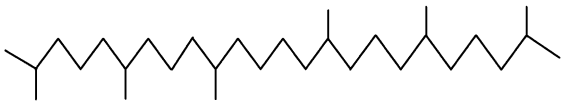

2, 6, 10, 15, 19, 23 hexamethyl tetracosane
(Squalane)

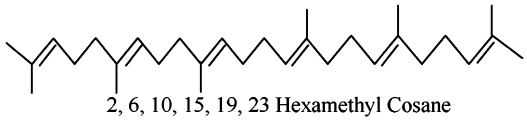

2, 6, 10, 15, 19, 23 Hexamethyl Cosane
(Squalene)

In the present contribution, studies on the nonaqueous phase behavior of monoglycerol fatty acid esters (monoglycerides) in different nonpolar oils (liquid paraffin (LP 70), squalane, and squalene) are reported. Formation of reverse rodlike micelles at elevated temperatures in the monoglyceride/oil systems are confirmed by X-ray scattering techniques. The effect of temperature, hydrocarbon chain length of surfactant, surfactant concentration, oil, and added water on the structure of the aggregate is also discussed.

2. Experimental Section

2.1. Materials. The commercial grade monoglycerol fatty acid ester surfactants glycerol α-monooctanoate (monocaprylin, Sunsoft 700P-2), glycerol α-monodecanoate (monocaprin, Sunsoft 760), and glycerol α-monododecanoate (monolaurin, Sunsoft 750) and the highly pure nonpolar oils liquid paraffin (LP 70), squalane, and squalene are kindly obtained from Taiyo Kagaku Company, Japan. The purities of monoglycerol fatty acid ester are 90.9% for monocaprylin, 91.1% for monocaprin, and 94.5% for monolaurin. The main impurities present are glycerol and difatty acid esters. Glycerol and difatty acid esters contamination are, respectively, 2.7% and 6.4% in monocaprylin, 3.1% and 5.8% in monocaprin, and 1.2% and 4.3% in monolaurin. The surfactants were used without further purification. All the nonpolar oils used are 99.5% pure by the gas chromatography test. The schematic molecular structures of monolaurin, squalane, and squalene are presented in Scheme 1.

2.2. Methods. *2.2.1. Sample Preparations*. To construct the phase diagram by visual observation, different samples with the compositions ranges from 2 to 100 wt % of surfactants were prepared in LP 70, squalane, and squalene in clean and dry glass ampules. The ampules were immediately flame-sealed, and the samples were mixed properly by using a dry thermo bath, vortex mixer, and repeated centrifugation to get the homogeneity. The phase behavior was studied over a wide temperature range (0−130 °C) at atmospheric pressure, keeping the samples inside the temperature control water bath or glycerol bath. The samples were left for at least 40−45 min at each temperature to equilibrate before observing the phase. The optical properties of the samples (birefringence) were identified with the crossed polarizer. Samples were prepared in 10 mL glass ampules for the small-angle X-ray scattering (SAXS) measurements and kept in the water bath at 60 °C for 1 h before measurement.

2.2.2. SAXS Measurements. SAXS measurements were carried out on monoglyceride/oil systems at elevated temperatures to study the structures of reverse micelles in the 5 wt % monoglyceride/oil systems. Additionally, the effects of temperature, surfactant concentration, and added water have systematically been examined.

For all SAXS measurements, we used a SAXSess camera (Anton Paar, PANalytical); a new and powerful updated version of the so-called Kratky compact camera, which is attached to a PW3830 laboratory X-ray generator with a long fine focus sealed glass X-ray tube (Kα wavelength of 0.1542 nm) (PANalytical) and operated at 40 kV and 50 mA. The SAXSess camera is equipped with focusing multiplayer optics and a block collimator for an intense and monochromatic primary beam with low background and a translucent beam stop for the measurement of an attenuated primary beam at $q = 0$. Samples were enclosed into a vacuum-tight thin quartz capillary with an outer diameter of 1 mm and a thickness of 10 μm, and the same capillary was used for all measurements to attain exactly the same scattering volume and background contribution. The sample temperature was controlled with a thermostated sample holder unit (TCS 120, Anton Paar). The scattered intensities were measured with an imaging plate (IP) detection system Cyclone (Perkin-Elmer, USA). Via SAXSQuant software (Anton Paar), two-dimensional intensity data were transformed to the one-dimensional scattering curves as a function of the magnitude of the scattering vector

$$q = \frac{4\pi}{\lambda}\sin(\theta/2) \tag{1}$$

where θ is the angle between the incident beam and the scattered radiation. All data were transmission-calibrated by normalizing an attenuated primary intensity at $q = 0$ to unity and were corrected for the background scattering from the capillary and the solvents. The absolute scale calibration was done using water as a secondary standard.

For monodisperse spherical systems, the total scattered intensity $I(q)$ involving n particles in unit volume can generally be given by

$$I(q) = nP(q)S(q) \tag{2}$$

where $P(q)$ is the averaged form factor and $S(q)$ is the static structure factor. For a dilute system, $S(q)$ is equal to one, and the $I(q)$ is simply given by $P(q)$. An expression similar to eq 2 can be applied to polydisperse spherical and nonspherical systems by replacing $S(q)$ by $S^{\text{eff}}(q)$.[17] $S^{\text{eff}}(q)$ is no longer only a function of the particle distribution in space but also depends on the form amplitudes of the particles. The average form factor $P(q)$ is given by the Fourier transformation of the pair-distance distribution function (PDDF), $p(r)$, as

$$P(q) = 4\pi\int_0^\infty p(r)\frac{\sin qr}{qr}\,\mathrm{d}r \tag{3}$$

The value $p(r)$ is directly linked to the convolution square of the spatially averaged electron density fluctuations,

$$\Delta\tilde{\rho}^2(r) = \langle\Delta\tilde{\rho}^2(r)\rangle = \left\langle\int_{-\infty}^{\infty}\Delta\rho(r_1)\Delta\rho(r_1 - r)\,\mathrm{d}r_1\right\rangle \tag{4}$$

where r corresponds to the distance between two scattering centers inside of the particle, and thus $p(r)$ contains information on the geometry of the particles in the real space.

The static structure factor $S(q)$ is given by the Fourier transformation of the total correlation function, $h(r) = g(r) - 1$, as

$$S(q) = 1 + 4\pi n \int_0^\infty [g(r) - 1] r^2 \frac{\sin qr}{qr} dr \qquad (5)$$

where g(r) is the pair correlation function. $S(q)$ describes the spatial distribution of the particles that highly differs depending on the interparticle interaction potential. Even in the case of uncharged systems, when the particle density is relatively high (>1 wt %), its contribution is not negligible.

The SAXS data for the reverse micellar solutions were analyzed by the generalized indirect Fourier transformation (GIFT) technique.[18,19] In the limited cases of well-defined colloidal systems, $P(q)$ may be fixed from a measurement at very low concentration or theoretical calculation, and the experimental structure factor, $S(q)^{exp}$, can be deduced by dividing the normalized scattered intensity, $I(q)/c$, by the defined $P(q)$.[20] However, for self-assemble systems such as micellar solutions and microemulsion droplets, $P(q)$ is a function of concentration and temperature and is determined from experiments.

GIFT attempts to determine $P(q)$ and $S(q)$ simultaneously with minimal assumptions, letting $P(q)$ be model-free in combination with an appropriate choice of the interparticle interaction potential model and the closure relation for the calculation of $S(q)$. In the calculation, we used a model of the averaged structure factor for a hardsphere (HS) interaction, $S(q)^{av}$,[21,22] which considers the Gaussian distribution of the interaction radius σ for individual monodisperse systems to account for polydispersity μ, together with the choice of a Percus−Yevick (PY) closure relation to solve the Ornstein−Zernike (OZ) equation. The detailed theoretical description on the method has been reported elsewhere.[23,24] Note that when the particle geometry deviates from an ideal spherical symmetry, the output parameters from $S(q)$ analysis become obscure and no longer exact. Nevertheless, the GIFT approach efficiently suppresses the influence of the interparticle interference scattering on the calculation of $p(r)$, and allows us to deduce a realistic $p(r)$.

2.2.3. Densimetry. Using a high precision DSA5000 densimeter (Anton Paar, Austria),[25] density measurements were carried out on monoglycerol fatty acid ester surfactants, oils (LP 70 and squalene), and the mixtures at the same temperature of SAXS measurements. The instrument is based on the conventional mechanical oscillator method, which measures the natural resonant frequency of a U-shaped glass tube filled with 1 mL of sample. The highly tuned temperature control of the apparatus makes an accuracy of 10 mK in an absolute value possible.

3. Results and Discussions

3.1. Phase Behavior. Binary phase diagrams of monoglycerol fatty acid esters surfactants in different nonpolar oils, namely LP 70, squalene and squalane, in the whole composition range at atmospheric pressure are shown in Figure 1.

At lower temperature, surfactant solid and oil phases are in equilibrium. Upon increasing the temperature, the surfactant solid melts at temperatures depending mainly on the lipophilic chain length of surfactant. Upon an increasing hydrocarbon chain of the surfactant, the solid to liquid transition temperature was monotonically increased, but the melting temperature of the solid phase was almost constant at all compositions. As is evident from Figure 1, monoglycerides, which have only one glycerol unit as a hydrophilic moiety in their molecules, do not form liquid crystalline phase in the nonpolar oils. Instead, the solid surfactant melts to form an isotropic single- or two-liquid-phase system depending on the systems and composition. However, in the surfactant/oil systems of diglycerol fatty acid esters, which have similar structures as monoglyceride but an additional glycerol moiety in their headgroup, solid surfactant transforms to the single L_α phase or the L_α + oil phase, which transforms to single or two-liquid phase with increasing temperature.[16] Because of a small headgroup in their molecules, monoglycerides cannot form an aggregate with a flat interface (lamellar structure), instead, they form isotropic solutions of small reversed aggregates.

The turbid solutions are obtained in the two-liquid phases region in all the monocaprylin/oil and also the monocaprin/squalane systems above the solid melting temperatures, and these separate into two transparent liquid phases on standing for few minutes. Judging from the solubility curve, one phase is an oil-rich phase with less surfactant and the other phase is the surfactant rich phase containing a considerable amount of oil. The size of the two-liquid phases domain was found to be dependent on the hydrocarbon chain length of the surfactant and the nature of oils. The width of domain of the two-liquid phases in the phase diagram (Figure 1) determines the miscibility of surfactants in oils. In the case of same surfactant monocaprylin, it is most miscible with squalene (the narrowest two-liquid phase domain among all) and least miscible with squalane (the widest two-liquid phases domain).

With increasing alkyl chain length the surfactants become increasingly lipophilic, and therefore, more miscible with oil, which is clearly evident from the comparison of phase diagrams (Figure 1). In contrast to monocaprylin, monocaprin in LP 70 or squalene as well as all the monolaurin/oil systems at higher temperatures forms a single isotropic solution at all compositions although monocaprin forms a turbid two-phase solution with squalane, which has the lowest miscibility with the surfactant.

The two-liquid phase transforms to a single phase isotropic solution upon further increasing the temperature. Two-phase to single phase transition temperature is the highest for the least miscible surfactant-oil system, that is, the monocaprylin/squalene system. The upper critical solution temperature of the monocaprylin/squalane system could be more than 120 °C and is not included in the phase diagram. The boundary between the single and two-phase regions corresponds to the cloud-point curve for a water−poly(oxyethylene) type of surfactant system,[26−30] in which the surfactant becomes less hydrophilic with increasing temperature, and ultimately the surfactant-rich phase separates out from the solvent-rich phase. In the oil systems, however, the penetration of oil in the surfactant chain increases and the miscibility of oil and surfactant increases with increase in temperature. Consequently, the phenomenon opposite to clouding occurs; that is, an isotropic solution of reversed aggregate is formed.

3.2. Effects of Temperature on the Micellar Structure. When amphiphilic molecules are added into the nonpolar organic solvents, the hydrophilic part of the amphiphile tends to avoid contact with the nonpolar environment, and like in conventional micelles in aqueous systems it is the hydrophobic effect that is the driving force for the aggregation of reverse micellar structure in nonpolar media with the headgroup oriented toward each other in the interior of the structure and with the hydrophobic groups oriented toward nonpolar solvent. In the reverse micellar aggregates, it is possible that the dipole−dipole interactions may hold the hydrophilic headgroups together in the core. Change in the concentration of surfactant, temperature, and additives in the liquid phases and structural groups in the surfactant may cause modulation of the size, shape, and aggregation number of the micelle, with the structure varying from spherical to rodlike or disklike lamellar.[31] Variation of the size of aggregates present in the isotropic solution of monoglyceride/oil systems as obtained from SAXS is discussed below.

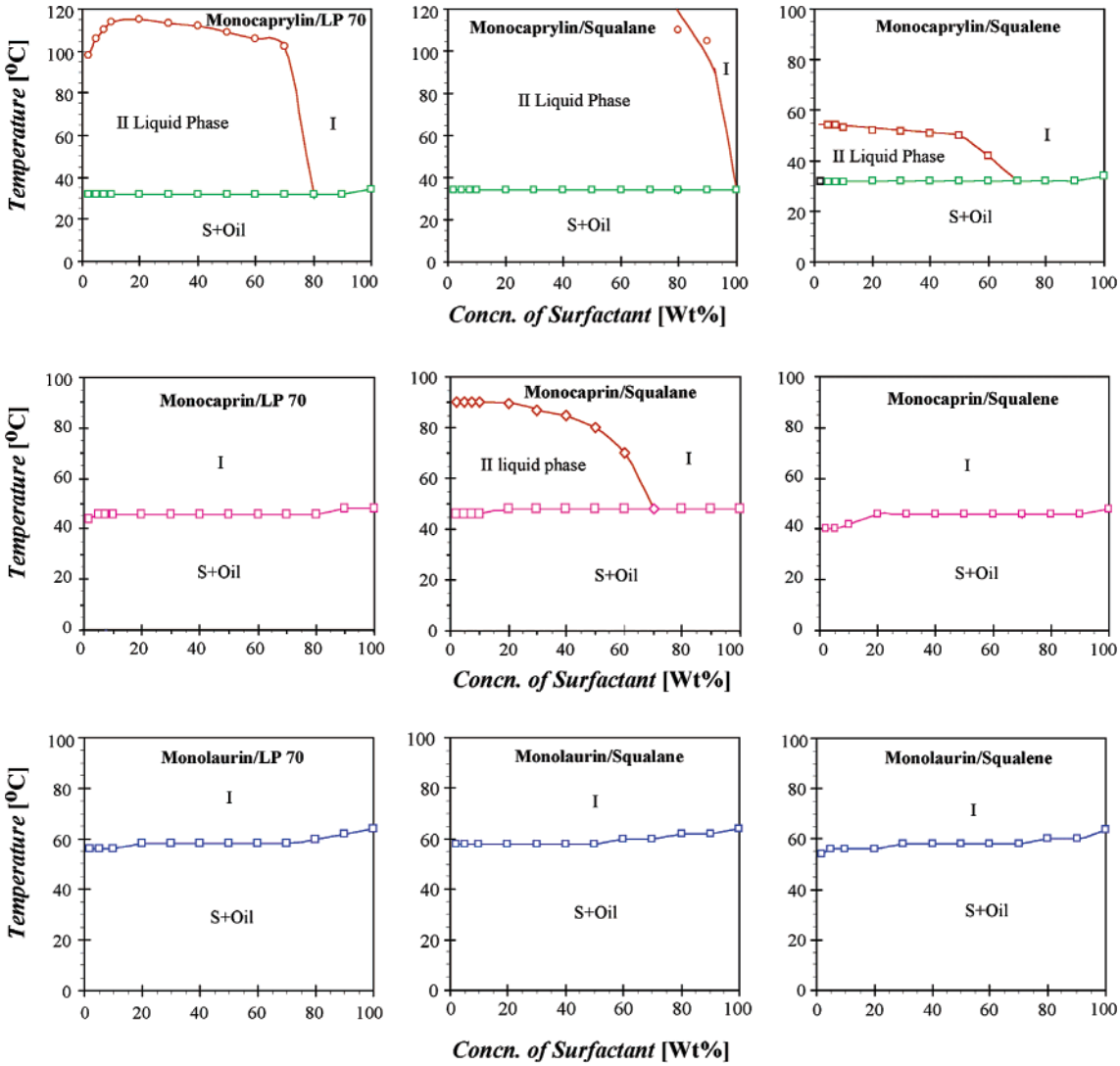

Figure 1. Phase diagrams of homologous series of monoglycerol fatty acid ester surfactants in different nonpolar oils, LP 70, squalane, and squalene (S = solid, I = isotropic single liquid phase).

In Figure 2 we display the scattering functions, $I(q)$, and the resulting $p(r)$ for the 5 wt % monocaprin/LP 70 system at different temperatures. The decreasing low-q slope of $I(q)$ and the resulting decrease in D_{max} with the rise of temperature provide direct evidence for decreasing micellar size with increasing temperature; the scattering intensity in the forward direction monotonically decreases with increasing temperature without changing high-q values, or in other words, the low-q slope of $I(q)$ increases with decreasing temperature as shown in Figure 2a. Growth to a longer rodlike particle typically leads to this kind of behavior.[19] As shown in Figure 2b, all PDDF curves exhibit a sharp peak in the low-r region and an extended tail to the high-r side, which is the typical feature of an elongated rodlike particle with nearly homogeneous electron density distribution. The inflection point that appears on the slightly higher r-side of the maximum in the PDDF curves semiquantitatively gives the cross section diameter of the hydrophilic core, which is well fitted to the twice the length of monoglycerol moiety. This cross section diameter is almost unchanged at all temperatures studied. On the other hand, the maximum dimension of the elongated particles, D_{max}, decreases from around 24 to 18 nm upon increasing temperature from 50 to 60 °C.

Unlike the case of aqueous surfactant systems, the miscibility of solvent and surfactant increases in surfactant oil systems with the rise of temperature because the surfactant molecules become increasingly lipophilic. The increased solubilization may also be due to increased thermal agitation, which would increase the space available for the solubilization in the micelle. With increasing temperature, the penetration of oil in the surfactant chain increases and the packing parameter decreases in consistence with the penetration model of Ninham and co-workers.[32,33] Therefore, the length of the cylindrical aggregates decreases, which is essentially a rod−sphere type of transition in the micellar shape. Besides, increasing temperature increases the surfactants hydrophobic character, the van der Waals interaction between the hydrocarbon chain of surfactant and oil increases, and this eventually increases the oil solubilization capacity of the surfactant. This is in good agreement with the phase behavior; more and more oils are solubilized at higher temperature as shown in Figure 1. Moreover, increasing temperature decreases the aggregation number in nonpolar media,[34] and less elongated or spherical particles are favored at elevated temperatures.

3.3. Effects of Alkyl Chain Length of Surfactant. The scattering functions, $I(q)$, and the corresponding PDDFs, $p(r)$, for 5 wt % monocaprin and monolaurin in squalene at 60 °C are shown in Figure 3. The data provide direct evidence for micellar elongation (an increase in D_{max} with an extended tail in $p(r)$) with decreasing the hydrocarbon chain length of monoglyceride). This result is in agreement with the phase

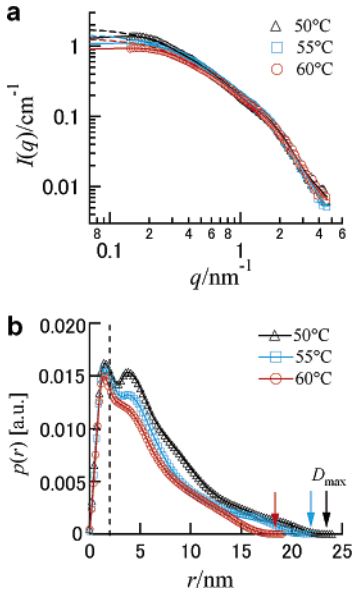

Figure 2. The X-ray scattered intensities $I(q)$ of 5 wt % monocaprin/LP 70 in absolute unit at different temperatures (a) and the pair-distance distribution functions (PDDFs) $p(r)$ extracted from these scattering curves with GIFT analysis (b). Solid and broken lines in panel a represent GIFT fit and the calculated (total) form factor for n particles existing in unit volume, $nP(q)$, respectively. The arrows in panel b indicate the maximum dimension of micelles, D_{max}, and the broken line on the inflection point of $p(r)$ after the maximum highlights the core diameter.

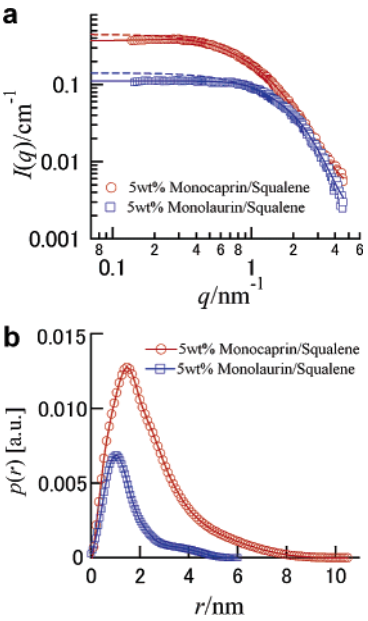

Figure 3. The X-ray scattered intensities $I(q)$ (a) and the corresponding $p(r)$ (b) for 5 wt % monocaprin/squalene and monolaurin/squalene systems at an elevated temperature, 60 °C. Solid and broken lines in panel a represent GIFT fit and the calculated (total) form factor for n particles existing in unit volume, $nP(q)$, respectively.

diagrams. Namely, the short-hydrocarbon chain surfactant tends to separate from oil as shown in Figure 1, resulting in the reduction of surface area per surfactant on the micellar hydrophobic/hydrophilic interface.

Compared to aqueous systems, much less is known regarding aggregation numbers of the micelles in nonpolar media, and some of it is controversial. However, from the data available, the average aggregation number in nonpolar media increases with an increase in dipole−dipole attraction or intermolecular bonding between the polar headgroups, and this decreases with

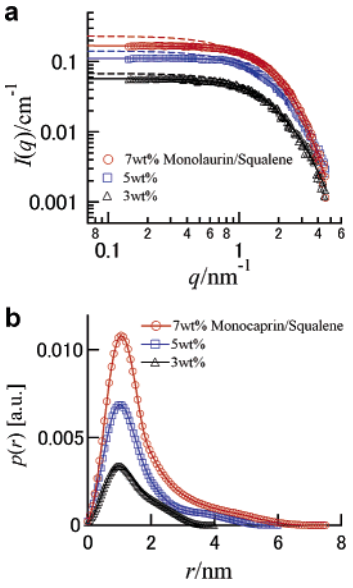

Figure 4. The scattering curves $I(q)$ of the monolaurin/squalene systems at different surfactant concentrations obtained on absolute scale (a), and the resulting pair−distance distribution functions (PDDFs), $p(r)$ (b). Solid and broken lines in panel a represent GIFT fit and the calculated (total) form factor for n particles existing in unit volume, $nP(q)$, respectively.

increase in the length of the hydrocarbon chain of the surfactant, number of carbon chain per surfactant molecule, the steric requirements of the chain close to polar headgroups, and the temperature.[34] In the present investigation we observed the decrease in the micellar size with increasing the hydrocarbon chain of the surfactant molecules. Thus our present result supports the theory of Ruckenstein and co-workers[34] that predicts a decrease in the aggregation number with the increasing hydrocarbon chain of surfactants.

3.4. Effect of Surfactant Concentration on the Micellar Growth. Micellar growth is a common phenomenon, and for ionic surfactants concentration, cosolutes, temperature, and others influence the growth. Poly(oxyethylene) type nonionic surfactants also show growth with increasing concentration depending on the polar headgroup. Like conventional poly(oxyethylene) type nonionic surfactants, monoglycerol fatty acid ester surfactants also give growth with concentration. Figure 4 shows the scattering functions, $I(q)$, and the corresponding PDDFs $p(r)$, for a monolaurin/squalene system at 60 °C and different surfactant concentrations. We observed the evidence for an increase in the maximum dimension of the micellar structure. That is, D_{max} is increasing with the surfactant concentration.

As shown in Figure 4b, all PDDF curves exhibit the typical feature of an elongated rodlike particle in view of a pronounced peak in the low-r region and an extended tail to the high-r side. The absence of local maximum and minimum on the lower-r side indicates nearly homogeneous electron density distribution (no core−shell structure) in scattering particles. Note that, since the scattering length density for oils and that for the hydrophobic part of surfactants are considered to be almost identical, SAXS can detect only the hydrophilic core of the reverse micelles. As can be seen from Figure 4a, increasing surfactant concentration increases the total scattering intensity. Besides this simple expected behavior due to the increased number density of the scattering objects at higher concentrations, more importantly we observed the more extended tails of $p(r)$ at higher concentrations (Figure 4b). This indicates the pronounced elongation in the micellar shape or, in other words, an increase in aggregation

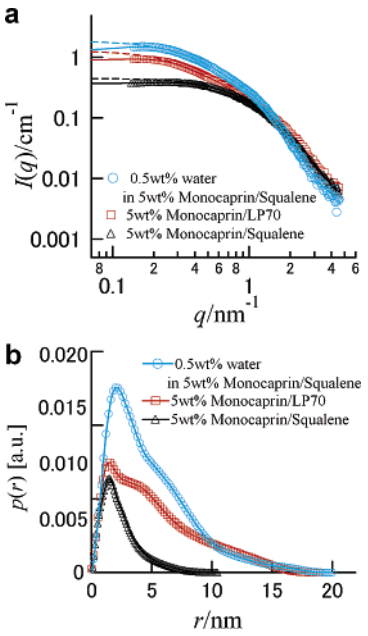

Figure 5. The scattered intensities $I(q)$ of 5 wt % monocaprin/squalene, monocaprin/LP 70 and 5 wt % monocaprin/squalene with added 0.5 wt % water obtained in absolute unit (a), and the corresponding PDDFs, $p(r)$, (b). Solid and broken lines in panel a represent GIFT fit and the calculated (total) form factor for n particles existing in unit volume, $nP(q)$, respectively.

number, with an increase in surfactant concentration. This behavior is similar to that observed in surfactant/water systems, where the micellar growth with increasing surfactant concentration is caused by entropy effects. Therefore, the micellar growth (sphere-to-rod transition) is expected to occur in conventional as well as in the reverse micellar system.

3.5. Effect of Oil and Addition of Water. In the present investigation, we found that micellar growth is favored on changing oil from squalene to LP 70. The scattering functions, $I(q)$, and the resulting $p(r)$ for monocaprin/squalene and monocaprin/LP 70 systems at 60 °C are displayed in Figure 5. $I(q)$ for the monocaprin/LP 70 shows a greater low-q slope than the monocaprin/squalene, whereas the drop appears in $q < \sim 0.2$ to 0.3 nm^{-1} because of an interparticle interference effect. This corresponds to an enhanced one-dimensional micellar growth in the former system,[19] which is also evident from the corresponding PDDFs shown in Figure 5b. In the squalene system, where shorter rodlike aggregates are formed, the mutual dissolution of surfactant and oil is the highest among three oils. The present result shows that when the mutual miscibility of surfactant/oil increases, the aggregates become shorter. This fact, supported by the effect of temperature and lipophilic chain length on the micellar size discussed above, may be explained in terms of the increased penetration of the miscible oil in the lipophilic layer of the aggregate.

It is well known that a small amount of water induces micellar formation in nonaqueous media in poly(oxyethylene) type nonionic surfactant systems. Even when surfactant aggregation does not occur or the aggregation number is considerably small in a particular solvent in the absence of other material, the addition of an insoluble solvent like water may give rise to aggregation with consequent solubilization of the additives.[35] The addition of water is expected to increase the spontaneous curvature as a result of increased headgroup repulsion. Besides, the added water solubilized in the interior of the micelle core in the nonpolar medium has been shown to cause an increase in the aggregation number.[36] Upon the addition of 0.5 wt % of water to a 5 wt % monocaprin/squalene system, the dramatic elongation of reverse micelles takes place, as proven by Figure 5b. A shift in the position of the inflection point after the maximum of the PDDF to the higher r-side indicates an increase in the cross-sectional diameter of the hydrophilic core. Hence, the data provide the direct structural evidence, showing that added water induces drastic elongation and simultaneously a slight expansion of the core diameter of the reverse micelles, and this is in good agreement with the finding of our previous work.[16]

It is still a matter of debate whether reversed aggregates can be formed in the absence of water. In the present surfactant system, reversed aggregates are formed without adding water. However, we cannot exclude the possibility of the presence of traces of water in the surfactant, as it is practically difficult to remove water completely and to measure SAXS data in an absolutely dry state.

3.6. Model Calculation of the Scattering Function. A model-independent approach like IFT (or its extended version of GIFT) and a modeling method based on the fitting analysis of the experimental scattering function with a theoretical scattering function calculated from plausible structure models basically give us complementary information on the structures if these procedures are done in the appropriate manner. We have tested a number of plausible structure models for the investigated reverse micelles, such as homogeneous and inhomogeneous (core−shell) cylinders or prolate globular particles. The theoretical scattering functions were calculated based on the method reported elsewhere[37] and fitted to the experimental scattering functions. To fix the scattering length density of the micellar core and shell, densities of the investigated mixtures, pure surfactants, and oils were measured at the same temperatures of SAXS measurements.

For instance, the densities of LP 70, squalene, monocaprin, and monolaurinare are, respectively, 0.8073, 0.8352, 0.9473, and 0.9193 g/cm^3 at 60 °C. These values result in the partial electron density of the hydrophilic part of monocaprin and monolaurin, 416 and 393 el/nm^3, respectively, for which the electron density of hydrocarbon group was calculated from the literature data.[38] The electron density differences $\Delta\rho$ (contrast) of the hydrophilic core are estimated to be 138.4, 134.6, and 111.6 el/nm^3, respectively, for monocaprin/LP 70, monocaprin/squalene, and monolaurin/squalene. As for the water added monocaprin/squalene system, the averaged $\Delta\rho$ was used for the micellar core accounting for the electron density of water being equal to 330.4 el/nm^3 at 60 °C, and the volume fraction of the hydrophilic part being 1.48% and that of water being 0.422%, which gives $\Delta\rho = 115.5$ el/nm^3.

It was not possible to detect any scattering length density difference between the micellar hydrophobic shell and the solvent oil from the modeling approach using core−shell structure models, as expected from nearly identical electron densities for surfactant hydrophobic group (hydrocarbon) and used oils. Therefore, the number of the adjustable parameters in the fitting procedure is essentially reduced to three: the core radius R, the total axial length L for a cylinder (or the short and long axes of a spheroid, a and b), and the number of aggregates n in unit volume. The number of surfactant molecules in a unit volume, N, divided by the extracted n gives the aggregation number N_{agg}.

We found that the form factor of the monoglyceride fatty acid ester/LP 70 system can on the whole be explained by the homogeneous cylinder model for the micellar hydrophilic core, whereas the small features cannot perfectly be reproduced by

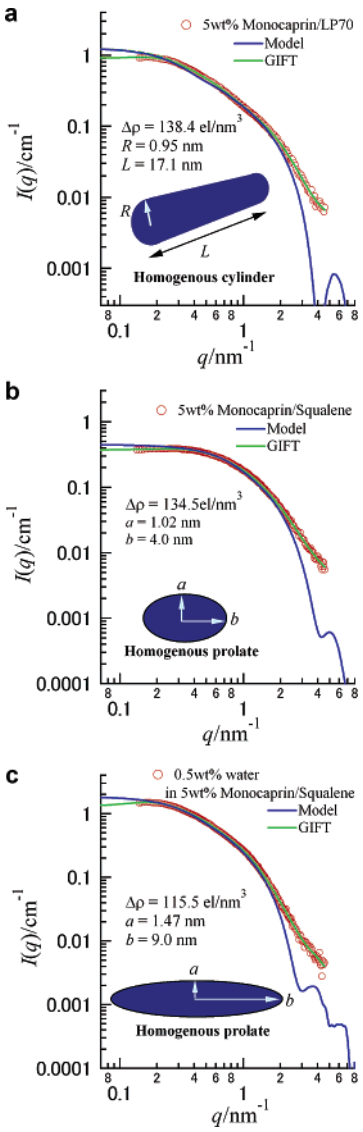

Figure 6. The model analysis of the X-ray scattered intensities of 5 wt % monocaprin/LP 70 (a), 5 wt % monocaprin/squalene (b), and 5 wt % monocaprin/squalene with added 0.5 wt % water (c). The data were fitted using models of a homogeneous cylinder with hemisphere endcaps for representation a and a homogeneous prolate for representations b and c.

such a simple model assuming a perfectly homogeneous electron density distribution and smooth and rigid interface. For all the LP 70 based systems, nearly constant values of ~0.9 to 1.1 nm were required for the core radius to reproduce the overall features of the experimental scattering functions, despite the variation of the axial length for different hydrocarbon lengths and temperatures. The form factor of the monoglyceride fatty acid ester/squalene systems can also be fitted with an elongated structure model with homogeneous density distribution, but it appears that a prolate structure rather than a cylinder gives the better results. The experimental $I(q)$ lacks a theoretically predicted minimum at $qR = 3.83$, where R is the section radius. Although this may partly be due to the experimental broadening effect, a nearly homogeneous but moderate electron density distribution within the core can hinder the appearance of the clear minimum. It is not able to improve the high-q deviation between the data and the theoretical function without considering a small continuous electron density distribution in the hydrophilic core.

The accuracy of our absolute intensity calibration is better than 10%, which means that the present N_{agg} analysis inherently

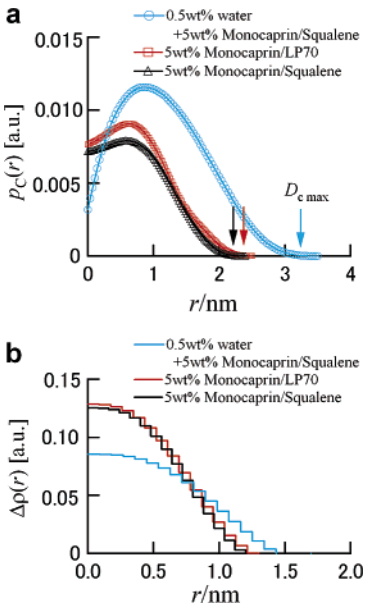

Figure 7. The model-independent core structure analysis for the micellar cross section. The cross-section PDDFs, $p_c(r)$, for monocaprin/LP 70, monocaprin/squalene, and water/monocaprin/squalene (a), where $D_{c\,max}$ highlighted by arrows gives the maximum core diameter. The cross section (core) radial electron density profiles, $\Delta\rho_c(r)$, deconvoluted from $p_c(r)$ (b) are shown.

includes the error of ~10%, excepting the errors from the misestimation of the geometrical parameters in the fitting procedure and the deviation of too simplified structure models from the actual structure of micelles. Nevertheless, an N_{agg} of ~260 is deduced for monocaprin/LP 70 at 60 °C, which goes up to ~330 at 50 °C. In contrast, the monocaprin/squalene system gives a considerably smaller N_{agg} value of 103 at 60 °C, but the addition of 0.5 wt % water drastically increases the value up to ~390. The 3 wt % monocaprin/squalene gives an N_{agg} value of ~27, which increases to ~37 for 5 wt % and reaches ~43 at 7 wt %. All these results and tendencies are consistent with those obtained with GIFT analysis.

3.7. A Model-Free Cross-Section Analysis. Our primary strategy is to extract the structural information of the investigated systems as model-independently as possible as we have shown in Figures 2−5; when the scattering objects are cylindrical (the axial length of a cylinder is at least 3 times greater than the cross section diameter) and the scattering length density profile of the cross section can be regarded simply as a function of the radial position, a model-free approach to the micelle cross-section structure becomes possible. In view of the $p(r)$ shown in Figures 2−5, the core diameter for all monoglyceride/oil systems, except a water-added one, is approximately in the range of 1.9−2.4 nm if judged from the inflection point after the sharp maximum of $p(r)$. The total (axial) length estimated from D_{max} is greater than the core diameter by a factor of at least 5 in most cases. Therefore, the investigated systems satisfy the requirement of the above model-free approach for the section structure.

The relation between the cross section radial density profile $\Delta\rho_c(r)$ and the cross section PDDF $p_c(r)$ is given by[39]

$$p_c(r) = r\Delta\tilde{\rho}_c^{\,2}(r) \tag{6}$$

Without imposing any structure model, the cross-section PDDF can be calculated from the experimental scattered intensity $I(q)$ according to

$$I(q)q = \pi L I_c(q) = 2\pi^2 L \int_0^\infty p_c(r) J_0(qr)\, dr \qquad (7)$$

where $J_0(qr)$ is the zero-order Bessel function. The IFT approach based on eq 7 yields $p_c(r)$, and $\Delta\rho_c(r)$ can be calculated via the deconvolution procedure of $p_c(r)$.

Figure 7a shows that as readily expected from Figure 5b, the core diameter of the water added monocaprin/squalene system, giving the value of ~3.0 to 3.2 nm, is exceptionally greater than those of other water-free systems typically in the range of 2.2−2.3 nm. The radial electron density profiles $\Delta\rho_c(r)$ for the micellar core displayed in Figure 7b provide the more intuitive pictures. The always positive but smoothly varying density may offer one possible explanation for the lack of the distinct minimum of $I(q)$ at $qR = 3.83$. The model-independent deduced core radii of ~1.1 to 1.2 nm for monocaprin/LP 70 and monocaprin/squalene are quantitatively complementary with those obtained from the modeling method. The core radius of ~1.5 nm for the water-added system apparently exceeds the extended chain length of the hydrophilic monoglycerol group, which indicates the existence of a water pool in the innermost micellar core although within the resolution of our present SAXS measurements and analysis an expected gap between the electron densities for water and hydrated monoglycerol group is not clearly resolved.

4. Conclusion

Phase behavior and self-organized structures of monoglycerol fatty acid esters having different alkyl chain lengths in different nonpolar oils, LP 70, squalane, and squalene, have thoroughly been investigated. At low temperatures, two phases, solid and liquid, exist in the whole concentration range of mixing. Because of a small headgroup in their molecules, monoglycerides do not form a flat lamellar liquid crystalline structure, which is formed in diglycerol fatty acid ester/oil systems. Upon an increase in temperature, they either form isotropic solutions of reversed aggregates or two-liquid phases depending on the nature of the oil and the lipophilic chain length of the surfactant. An increase in temperature increases the solubility of surfactant in the oil, and the two-liquid phase equilibrium transforms to an isotropic single phase. This phase transition corresponds to the reverse of the cloud-point phenomenon observed in aqueous nonionic surfactant systems. The surfactants are the most soluble in squalene and the least soluble in squalane. Monoglycerides form reversed rodlike micelles at elevated temperatures, whose size decreases on increasing the temperature and the hydrocarbon chain length of the surfactant, which is in good agreement with the theory, which predicts a decrease in the aggregation number with increasing hydrocarbon chain. These results also confirm the validity of the penetration model of Ninham and co-workers in reversed surfactant systems. As has been expected, the micellar size monotonically increases with increasing surfactant concentration and also increases on changing oil from squalene to LP 70 in a particular surfactant/oil system. Dramatic elongation of the reversed rodlike aggregate can be induced by adding a small amount of water.

Acknowledgment. We dedicate this research article to Prof. Hironobu Kunieda who inspired us during the experimental work of this project but untimely passed away before the project was finalized. This work was partly supported by the CREST of JST Corporation. T.S. acknowledges a support from the 21st Century COE Program at Waseda University funded by the MEXT, Japan.

References and Notes

(1) Ekwall, P. *Advances in Liquid Crystals*; Brown, G. H., Ed.; Academic Press: New York, 1975; Vol. 1.
(2) Sjöblom, J.; Stenius, P.; Danielsson, I. In *Nonionic Surfactant*; Shick, M. J., Ed.; Marcel Dekker: New York, 1987; Vol. 23, p 370.
(3) Shinoda, K. *J. Colloid Interface Sci.* **1970**, *34*, 278.
(4) Lang, J. C.; Morgan, R. D. *J. Chem. Phys.* **1980**, *73*, 5849.
(5) Mitchell, D. J.; Tiddy, G. J. T.; Waring, L.; Bostock, T.; McDonald, M. P. *J. Chem. Soc., Faraday Trans.* **1983**, *79*, 975.
(6) Clunie, J. S.; Goodman, J. F.; Symons, P. C. *Trans. Faraday Soc.* **1969**, *65*, 287.
(7) Saito, H. *Nihon Kagaku Zasshi* **1971**, *92*, 223.
(8) Strey, R.; Schomäcker, R.; Roux, D.; Nallet, F.; Olsson, U. *J. Chem. Soc., Faraday Trans.* **1990**, *86*, 2253.
(9) Herrington, T. M.; Shali, S. S. *J. Am. Oil. Chem. Soc.* **1988**, *65*, 1677.
(10) Rodriguez, C.; Acharya, D. P.; Hinata, S.; Ishitobi, M.; Kunieda, H. *J. Colloid Interface Sci.* **2003**, *262*, 500.
(11) Stubenrauch, C. *Curr. Opin. Colloid Interface Sci.* **2001**, *6*, 160.
(12) Takagi, K.; Hirai, M.; Fujinuma, Y.; Fujimatsu, H.; Usami, H.; Ogasawara, S.; Kasahara, Y.; Yuki, A. *J. Oleo Sci.* **1995**, *44*, 207.
(13) Kunieda, H.; Uddin, Md. H.; Yamashita, Y.; Furukawa, H.; Harashima, A. *J. Oleo Sci.* **2002**, *51*, 113.
(14) Kunieda, H.; Kaneko, M.; Fujiyama R.; Ishitobi, M. *J. Oleo Sci.* **2002**, *51*, 761.
(15) Kunieda, H.; Uddin, Md. H.; Furukawa, H.; Harashima, A. *Macromolecules* **2001**, *34*, 9093.
(16) Shrestha, L. K.; Masaya, K.; Sato, T.; Acharya, D. P.; Iwanaga, T.; Kunieda, H. *Langmuir* **2006**, *22*, 1449.
(17) Weyerich, B.; Brunner-Popela, J.; Glatter, O. *J. Appl. Crystallogr.* **1999**, *32*, 197.
(18) Brunner, P. J.; Glatter, O. *J. Appl. Crystallogr.* **1997**, *30*, 431.
(19) Glatter, O.; Fritz, G.; Lindner, H.; Brunner, P. J.; Mittelbach, R.; Strey, R.; Egelhaaf, S. U. *Langmuir* **2000** *16*, 8692.
(20) Stradner A.; Sedgwick H.; Cardinaux F.; Poon, C. K. W.; Egelhaaf, S. U.; Schurtenberger, P. *Nature* **2004**, *432*, 492.
(21) Pusey, P. N.; Fijnaut, H. M.; Vrijm, A. *J. Chem. Phys.* **1982**, *77*, 4270.
(22) Salgi, P.; Rajagopolan, R. *Adv. Colloid Interface Sci.* **1993**, *43*, 169.
(23) Sato, T.; Hossain, Md. K.; Acharya, D. P.; Glatter, O.; Chiba, A.; Kunieda, H. *J. Phys. Chem. B* **2004**, *108*, 12927−12939.
(24) Acharya, D. P.; Sato, T.; Kaneko, M.; Singh, Y.; Kunieda, H. *J Phys. Chem. B* **2006,** *110*, 754.
(25) Fritz, G.; Scherf, G.; Glatter, O. *J. Phys. Chem. B* **2000**, *104*, 3463.
(26) Schick, M. J. *J. Colloid Sci.* **1962**, *17*, 801.
(27) Hey, M. J.; Ilett, S. M.; Davidson, G. *J. Chem. Soc., Faraday Trans.* **1995**, *91*, 3897.
(28) Tasaki, K. *J. Am. Chem. Soc.* **1996**, *118*, 8459.
(29) Karlström, G. *J. Phys. Chem.* **1985**, *89*, 4962.
(30) Kjellander, R.; Florin, E. *J. Chem. Soc., Faraday Trans. 1* **1981**, *77*, 2053.
(31) Winsor, P. A. *Chem. Rev.* **1968**, *68*, 1.
(32) Mitchell, D. J.; Ninham, B. W. *J. Chem. Soc., Faraday Trans. 2* **1981**, *77*, 601.
(33) Israelachvilli, J. N.; Mitchell, D. J.; Ninham, B. W. *J. Chem. Soc., Faraday Trans. 2* **1976**, *72*, 1525.
(34) Ruckenstein, E.; Nagarajan, R. *J. Phys. Chem.* **1980**, *84*, 1349.
(35) Kitahara, A. *Adv. Colloid Interface Sci.* **1980**, *12*, 109.
(36) Mathews, M. B., Hirschhorn, E. *J. Colloid Sci.* **1953**, *8*, 86.
(37) Glatter, O. *Acta Phys. Austriaca* **1980**, *52*, 243.
(38) Nagarajan, R.; Ruckenstein, E. *Langmuir* **1991**, *7*, 2934.
(39) Glatter, O. *J. Appl. Crystallogr.* **1980**, *13*, 7−11